3P3-5

Spurious Mode Suppression of First Symmetric Mode Lamb Wave Resonator by Modifying Wavelength

Ferriady Setiawan[1†*], Michio Kadota[1], and Shuji Tanaka[1*] ([1]Grad. School Eng., Tohoku Univ.)

1. Introduction

Plate wave devices using higher modes have been studied in recent years for high-frequency and wide-bandwidth (BW) mobile communication filters in 5G and beyond 5G operation.[1-6] The first anti-symmetric mode (A_1) resonator or also called laterally excited bulk acoustic resonator (XBAR) can achieve a high frequency of 5 GHz and 6 GHz, which has been aplied for Wi-Fi filters with large bandwidth exceeding 600 MHz or 1200 MHz.[3] Since then, the number of reports on the A_1 and higher order A mode Lamb wave resonators have been increasing in recent years. However, the higher the order of mode is, the BW will become narrower.[4]

Another mode of plate wave, the first shear horizontal mode (SH_1) has also been reported as it can achieve a high frequency of 3.2 GHz and a wide BW of 24.6% on a 0.57 µm thick $LiNbO_3$ (LN) thin plate.[5] However, the frequency is still not high enough for 5G filter operations. Another mode of Lamb wave, the first symmetric mode (S_1) was not much reported. Liu *et al.* reported an S_1 mode resonator on a 0.033λ thick X-cut LN thin plate with a frequency of 6.4 GHz, but the reported electromechanical coupling factor (k^2) is as low as 3.3%.[6]

This paper reports a high-frequency S_1 mode resonator on an LN thin plate with higher k^2 around 10%. This was achieved by selecting the optimal cut angle of LN. Also, spurious responses are reduced by using a suitable inter-digital transducers (IDT) wavelength (λ).

2. Simulation

The suitable cut angle for an S_1 mode resonator was determined by FEM simulation (FEMTET, Murata Software). **Fig. 1** shows the dependency of the phase velocity and k^2 on the second Euler angle θ of an LN thin plate with a thickness of 0.1λ. S_1 mode on (0º, 120º, 0º) LN exhibits a high phase velocity of more than 35 km/s, which is higher than those of A_1 and SH_1 modes. **Fig. 2** shows k^2 of S_1 mode on a 0.1λ thick LN as a function of θ with electrically free (red curve) and electrically short (green curve) bottom plane. S_1 mode has a high k^2 of 19.4% on (0º, 120º, 0º) LN with electrically short bottom plane like SH_1 mode.[5]

E-mail: †*setiawan.ferriady.r1@dc.tohoku.ac.jp

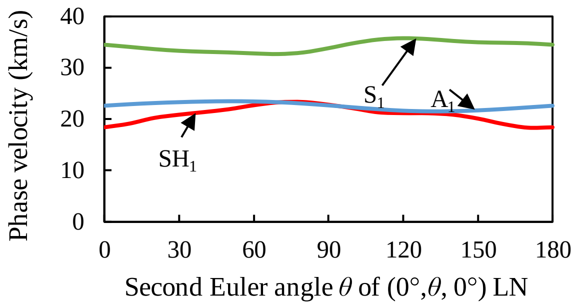

Fig. 1 Phase velocity of various modes of plate waves on LN with 0.1λ thickness as a function of Euler angle (0º, θ, 0º).

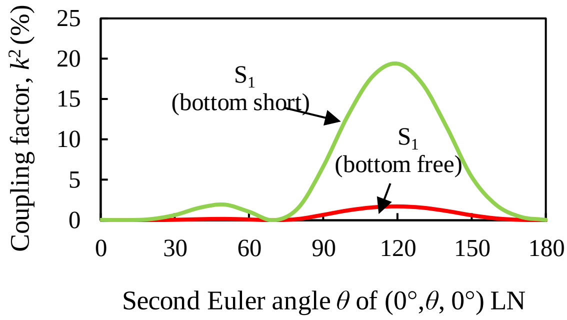

Fig. 2 Coupling factor (k^2) of S_1 modes of plate waves on 0.1λ thick LN with electrically free (red curve) and short (green curve) bottom plane as a function of angle (0º, θ, 0º).

The backside electrode was necessary to generate a symmetric electric field to excite the symmetric displacement.

The S_1 mode resonator composed of 80 nm thick Al IDT, a 0.5 µm thick (0º, 110º, 0º) LN plate, and an 80 nm thick Al bottom electrode were simulated. The spurious free characteristic was an important parameter for filter application. In Ref. 5, it was considered that a resonator with large metallization ratio (MR) and IDT λ can achieve a spurious free characteristic. Thus, the S_1 mode resonator with MR of 0.8 was considered to strengthen the electric field in the thickness direction. **Fig. 3** shows the simulated frequency characteristic at different IDT λ from 25 µm to 50 µm. S_1 mode was generated at frequency around 5 GHz regardless of λ. As the IDT λ increases, the in-band spurious responses become smaller and almost spurious-free characteristic was generated at IDT λ of more than 35 µm.

3. Fabrication and Measurement

Fig. 4 shows the S_1 mode Lamb wave resonator structure, which consists of 80 nm thick Al IDT, 0.6-0.7 µm thick (0º, 110º, 0º) LN plate, and 80 nm thick Al bottom short plane. The fabricated S_1 mode resonator had 5-8 pairs of Al IDT electrodes with a MR of 0.8, aperture of 5-9λ, and grating reflectors with 9-18 fingers on both sides of the IDT.

Fig. 5 shows the measured frequency characteristics of the fabricated S_1 mode resonators with IDT λ of 20 to 50 µm. The resonance frequencies (f_r) were measured at 3.05-3.92 GHz, while the anti-resonance frequencies (f_a) were measured at 3.4-4.31 GHz. The frequency was slightly lower than the simulated one because the resonator was fabricated on a thinner LN plate than the simulated one. The BW was 10%, which was larger than that reported in Ref. 6.

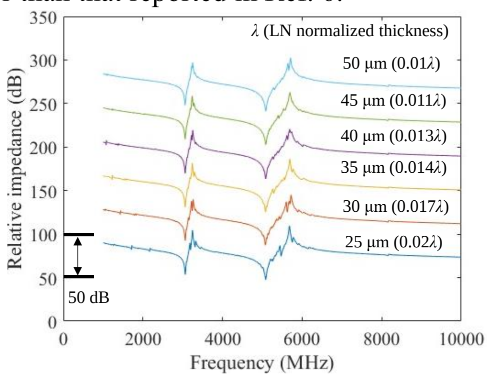

Fig. 3 Simulated frequency characteristics of S_1 mode resonators on a 0.5 µm thick (0º, 110º, 0º) LN with IDT λ of 25-50 µm.

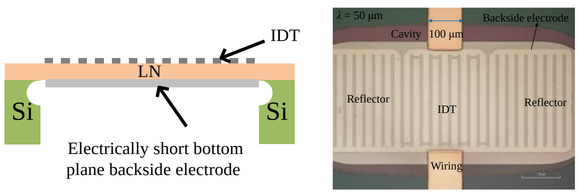

(a) (b)

Fig. 4 Structure of fabricated S_1 mode resonator. (a) Cross section and (b) top view.

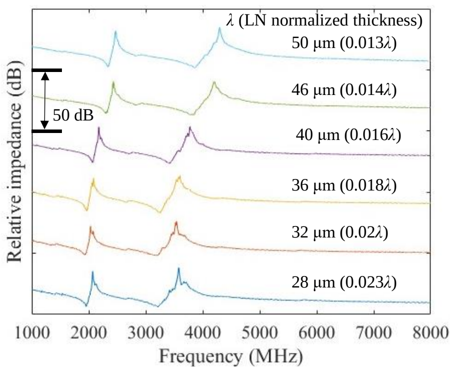

Fig. 5 Measured frequency characteristics of S_1 mode resonators on a 0.65 thick µm (0º, 110º, 0º) LN. MR = 0.8, Al IDT thickness = 80 nm, and λ = 4-50 µm.

The frequency characteristics also confirmed that the spurious free characteristic could be achieved with IDT λ larger than 36 µm (< 0.018λ LN normalized thickness). When the IDT λ becomes larger, the LN normalized thickness becomes smaller, and thus the frequency of spurious modes can be moved further away from the main response. However, the SH_1 mode spurious response was also generated around 2.5 GHz although the IDT λ was changed because it has a tendency like S_1 mode wave.

4. Conclusion

This paper reported the S_1 mode resonator on a (0º, 110º, 0º) LN thin plate with a large IDT λ to achieve a spurious-free characteristic. To preferentially excite the S_1 mode wave, an electrically short bottom plane opposite the IDT was needed. The S_1 mode resonator was fabricated with IDT λ of 28-50 µm, an Al IDT and backside electrode thickness of 80 nm, and a MR of 0.8. The measured frequency characteristics show that S_1 mode was generated around 3.5 GHz with wide BW of 10% on a 0.65 µm thick LN plate. The spurious free characteristic was obtained with IDT λ larger than 36 µm (< 0.018λ LN normalized thickness). This research demonstrated that S_1 mode resonator had the potential to be used for 5G new bands filter applications.

Acknowledgment

This research was partly supported by SCOPE #JP225002001 and JST SPRING, Grant Number JPMJSP2114. We would like to thank Dr. Hideki Takagi at the National Institute of Advanced Industrial Science and Technology (AIST) for the bonding of the wafers and Prof. Kenya. Hashimoto at University of Electronic Science and Technology of China for useful discussion.

References

1) M. Kadota, T. Ogami, K. Yamamoto, H. Tochishita, and Y. Negoro, IEEE Trans. Ultrason. Ferroelectr. Freq. Contr., 57 (2010) 2564.
2) V. Plessky, Proc. IEEE Int. Ultrason. Symp. (IUS), 2022, A3L-02-1004.
3) J. Koulakis, J. Koskela, W. Yang, L. Myers, G. Dyer, and B. Garcia, Proc. IEEE Int. Ultrason. Symp. (IUS), 2021, B3L-05-5015.
4) Y. Yang, R. Lu, L. Gao, and S. Gong, IEEE Trans. Microw. Theory Tech., 68 (2020) 5211.
5) F. Setiawan, M. Kadota, and S. Tanaka, Jpn. J. Appl. Phys., 63 (2024), 076505.
6) X. Liu, Z. Dai, Z. Su, and C. Zuo, Proc. IEEE/MTT-S Int. Microw. Symp. (IMS), 2023, pp. 899-902.